Large Area Plasma Processing System Based on Electron Beam Ionization

D. Leonhardt[1,*], C. Muratore[†], S. G. Walton[1], D. D. Blackwell[2], R. F. Fernsler[1] and R. A. Meger[1]

[1] *Naval Research Laboratory, Plasma Physics Division, Washington, DC 20375*
[2] *SFA, Inc., Largo, MD 20774*

Abstract
NRL has developed a number of hollow cathodes to generate sheets of high energy electrons, culminating in a 'Large Area Plasma Processing System' (LAPPS) based on the electron beam ionization process. In this work, we discuss (1) a large area (0.5 m x 1 m) plasma with a comparably large substrate stage and (2) various materials modification tests on smaller (20 cm x 30 cm) systems, both complemented by time-resolved, *in situ* plasma diagnostics (mass spectrometry, Langmuir probes, cathode currents). The materials' modification tests consist of polymeric material (photoresist) and silicon removal, and also nitriding of stainless steel. Results of *ex situ* materials analysis are used to qualify the processing capability and plasma source.

1. Introduction

Conventional discharges (such as dc/rf glows, capacitive, ECR, ICP) directly heat electrons with externally applied fields to ionize the gas, which results in a significant loss of input power to low-energy gas excitation processes rather than plasma production (ionization or dissociation). Hence, plasma electron temperatures are typically multiple electron volts, which translates to an environment of high plasma potentials (> 10 V), sheath drops and ion isotropy at surfaces. Plasmas produced by electron beams (e-beams) are quite different than conventional discharges. When a high energy beam of electrons passes through a gas, its dominant energy loss process is ionization of the gas followed by dissociation and finally inelastic excitations. Secondary electrons are created over a wide energy spectrum but cool rapidly through collisions with the background gas and thus the plasma electron temperature is low. Moreover, the direct ionization mechanism makes this plasma production process extremely efficient when compared to conventional plasma discharges. These attributes coupled with the independence of plasma gas composition and uniform scalability make e-beam produced plasmas well suited for materials applications, from surface activation of fragile polymer substrates to high energy reactive ion etching of hard semiconductor materials.

Electron beam ionization has been shown to be both efficient at producing plasma and scalable to large area (square meters). Fernsler [1] and Manheimer [2] *et al.* have discussed the detailed physics behind the plasma production mechanisms, which agree with *in situ* experimental measurements [3,4]. More recently, a broader view of e-beam produced plasmas was presented [5] to illustrate both the fundamental aspects and the range of plasma source configurations being investigated for various applications. This work reports on the recent experimental progress of some of the applications that are being pursued for materials' surface modification, and the development of a large area plasma processing system (LAPPS).

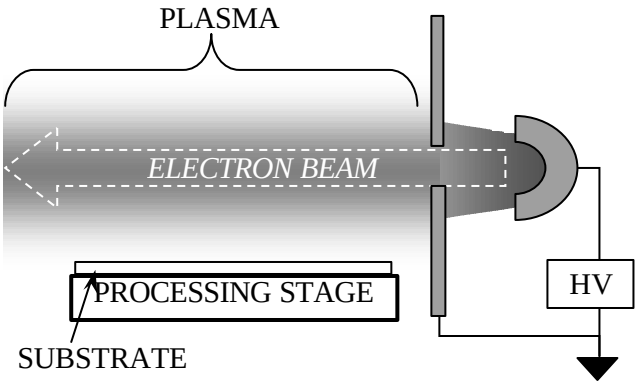

Figure 1 Electron-beam generated plasma in materials' processing arrangement.

2. Experimental Details

Generally, these systems consist of a pulsed, planar plasma generated by a magnetically collimated sheet of 2-3 kV, < 1 mA/cm^2 electrons injected into a neutral gas background (oxygen, nitrogen, sulfur hexafluoride, argon) with typical operating pressures in the range of 20 to 150 mtorr. The arrangement of the planar plasma processing

* Email: darrin@ccs.nrl.navy.mil
† ONR/ASEE Postdoctoral Research Fellow

system is shown in Fig 1. The processing stage (or substrate holder) was introduced laterally, to the 'face' of the plasma sheet. In the application tests, the stage was introduced at the middle of the 25 cm x 50 cm plasma sheets. Stage construction consisted of a 13 cm diameter electrode with grounded support structures, rf-bias and temperature control capabilities. All construction materials were stainless steel and machinable ceramic. Linear hollow cathodes operating at –2 kV with 0.5-10 ms pulse lengths and various duty cycles generated the electron beam, as described previously [6]. External magnetic fields of 150-165 Gauss collimated the e-beam to maintain a localized ionization region. All chambers were metal in construction and had base pressures below $2x10^{-6}$ Torr.

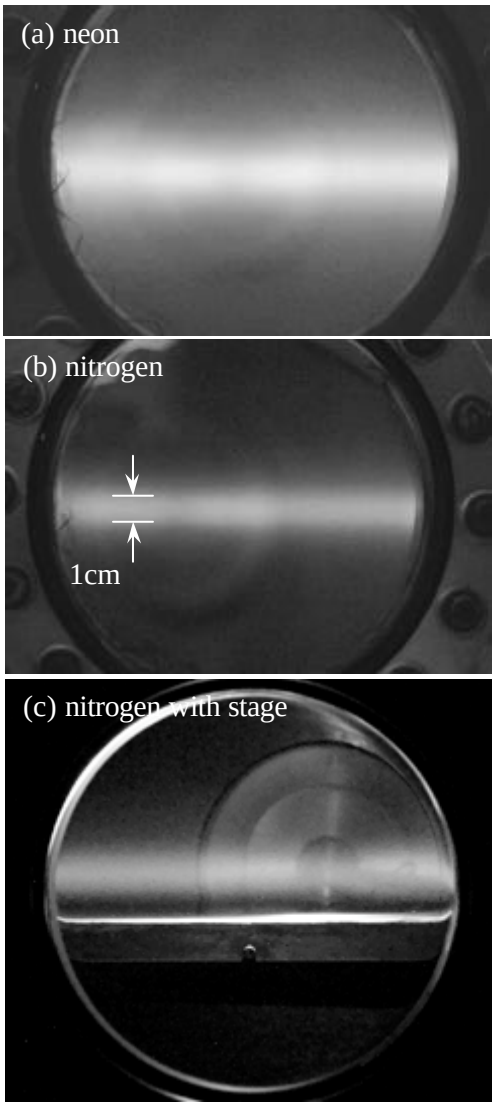

Figure 2 Large area plasma without stage (a) neon (b) nitrogen and with stage in (c).

The LAPPS hollow cathode was 50 cm long, providing a 50x1 cm^2 electron beam source which traveled the length of the chamber (~ 100 cm). Figure 2 shows a portion of this plasma source, photographed through a 20 cm viewport. In these photos, the 50 cm dimension goes into the page surface while the 100 cm dimension was along the page. The 1 cm beam thickness is marked in (b). Figure 2 shows a (a) 75 mT neon plasma, (b) 55 mT nitrogen plasma, and a (c) 55 mT nitrogen plasma with the large processing stage introduced. The processing stage was slightly wider than the plasma surface (~60x90 cm^2), and made similar to the smaller stages previously discussed. The stage is grounded in Fig 2c. With a cathode operating current of <100 mA/pulse, these plasmas had densities of $2\text{-}6x10^{11}$ cm^{-3} in the beam channel.

Applications

Polymeric and semiconductor samples were cut into ~ 1cm^2 pieces and mounted on the processing stage, which was positioned 1 cm from the e-beam edge. The processing stage was water cooled to keep the temperature at 20±4°C. In the etching tests, an rf-induced dc bias level (bias voltage) was applied to the processing stage to vary the incident ion energies during the plasma pulse. Etch rates (ER) were determined through stylus profilometry (Tencor P-10) or scanning electron microscopy (SEM) analysis and are calculated from the total plasma exposure time and not the actual laboratory time. The polymeric materials were industry standard negative or i-line photoresists, etched in O_2/Ar gases. Figure 3a shows the ER dependence for a negative resist as the bias voltage was varied. In these tests, plasmas were formed in 55 mTorr of pure oxygen (80 sccm). A moderately linear relationship between bias voltage and ER was seen, which increased strongly at higher voltages. Diluting the working gas with argon (keeping a fixed bias voltage of –50 V) resulted in the ER behavior shown in Fig 3b. From this data, the ER remained fairly constant until the oxygen percentage dropped below 20%. The total pressure of the mixtures was 65 mT, increasing to 70 mT for pure Ar.

Figure 4 shows the results from a feature cleaning test carried out in a pure O_2 plasma with a –50 V bias on the processing stage. The samples came from a commercial ashing process for Cu vias on i-line resist, shown by the SEM photo in Fig 4a. This photo shows residual spires coming from around the edges of a 300 nm via, left behind after the [cleaning] ash process. The SEM photo in Fig 4b shows removal of the residual spires after the 3-minute e-beam plasma exposure.

Mixtures of Ar or O_2 with SF_6 gas were used to etch crystalline <100> silicon. Figure 5 shows the measured etch rates with respect to the bias voltage for O_2/SF_6 mixtures (55/8 sccm) and Ar/SF_6 mixtures (35/15 sccm). Operating pressures were 60 and 70 mT, respectively. The O_2 plasma shows an increase in ER at V_{bias} > -100 V, but was generally an order of magnitude smaller than the Ar plasma for lower energies.

The Ar plasma ER varies strongly with the applied bias level, starting out slowly before rapidly increasing to ~ 1 micron/min at V_{bias} = -125 V.

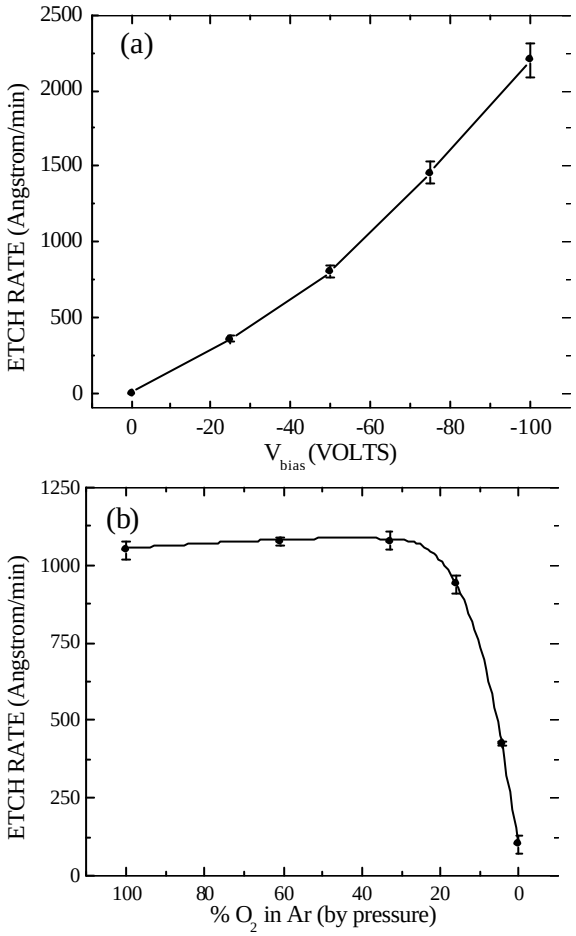

Figure 3 Etch rates of resist material with respect to (a) V_{bias} and (b) % O_2.

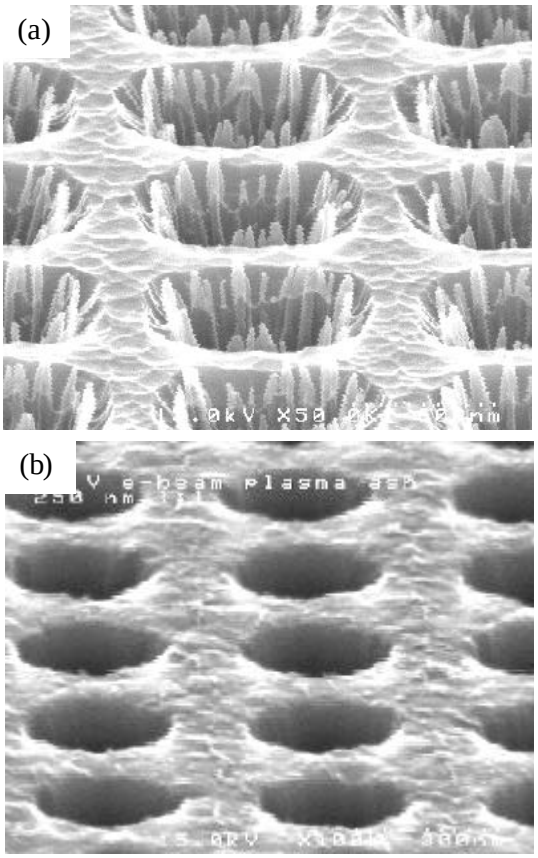

Figure 4 300nm via structures after standard ash process (a) before and (b) after a –50V_{bias} etch in O_2 plasma.

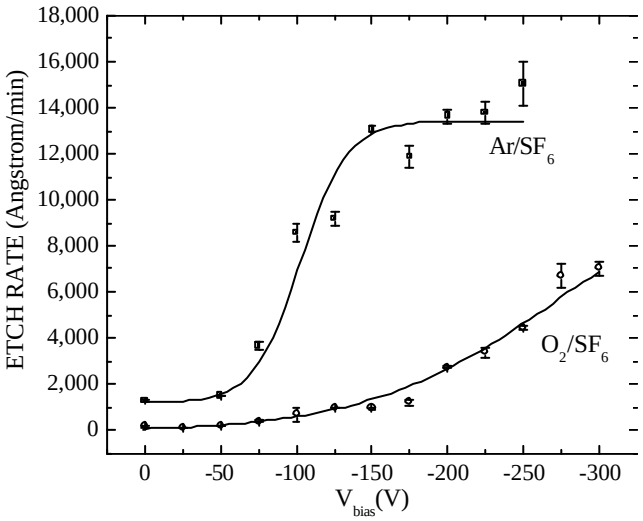

Figure 5 Silicon etch rate with respect ot bias voltage for O2/SF6 (55:8) and Ar/SF6 (35:15) mixtures.

Plasma nitriding experiments were carried out on 316 stainless steel substrates. Sample tiles, approximately 5x5 cm^2 were cut from a 02 cm thick plate and polished to a surface roughness of 7 nm. Samples were then heated to 340-440°C and cleaned in an Ar/H_2 plasma for 30 minutes before being exposed to a 60 mTorr N_2 plasma for 1.4 hours of plasma exposure. A constant –100 Vdc signal was applied to the processing stage for the cleaning and nitriding periods. Samples were allowed to cool, removed from vacuum and analyzed in the SEM to determine the surface nitride thickness. At 340°C, a 0.75 micron thick layer was observed, increasing to 1.3 microns at 400°C and 2.1 microns at 440°C. An Arrhenius plot of these growth rates and temperatures, gives a surface activation energy of 85 kJ/mole (0.90 eV) for this process.

The plasma diagnostics presented here consist of Langmuir probe and ion mass spectrometry measurements as discussed in References [3] and [4], respectively. The ion mass spectrometry provides information of the relative ion fluxes and their energies at the substrate, while the Langmuir probe data, taken at the center of the e-beam, provides plasma density, electron temperature and plasma potential. For the nitrogen plasma discussed previously, the temporally resolved plasma characteristics from these measurements are shown in Fig 6 for a 3 ms e-beam pulse with the grounded sampling stage (mass spectrometer in this case) located 1 cm away from the e-beam. The data shown in Fig 6 illustrates: (a) a rapid ion flux build up, particularly for the more energetic ions; (b) low energy atomic ions with a long decay after the e-beam was turned off but a rapid decay of molecular ion flux; and (c) a steady-state plasma electron densities of $2x10^{11}$ cm^{-3} and temperatures of 0.4 eV. The variation in ion flux with gas composition was also measured and is shown in Fig 7 for mixtures of argon and nitrogen. This data was time averaged and integrated over the entire ion energy distribution before normalized to the total ion flux. The dominant ion fluxes (N^+ and Ar^+) show a linear relationship with the concentration of their parent gas pressure.

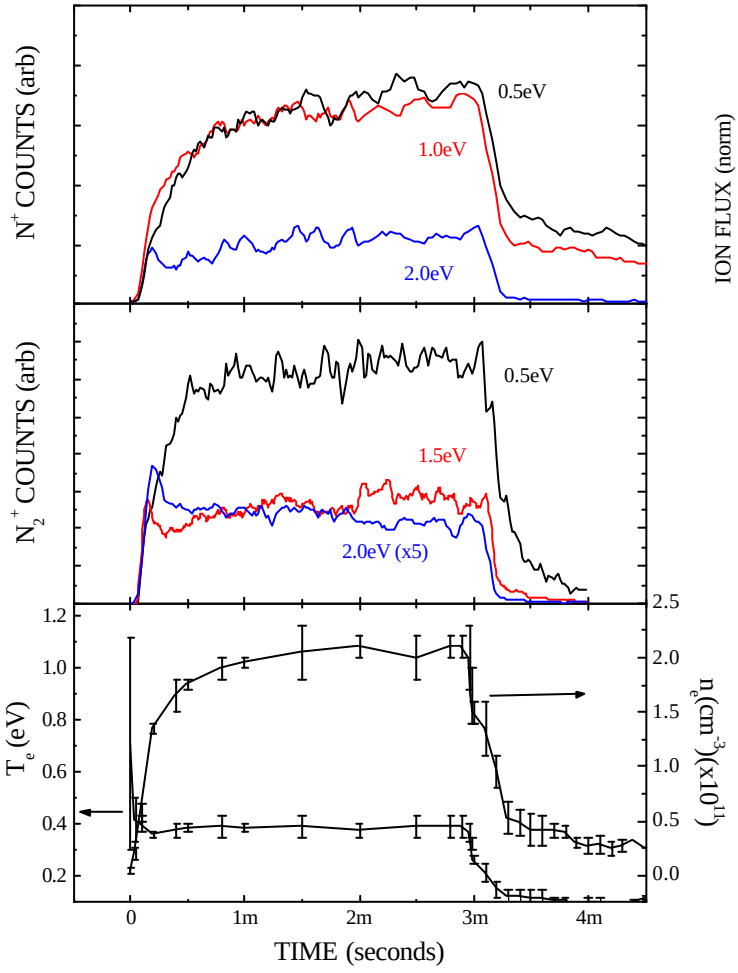

Figure 6 Temporally resolved ion fluxes and bulk plasma characteristics. Flux measurements are made at fixed energy analyser settings. The plasma pulse length was 3 ms.

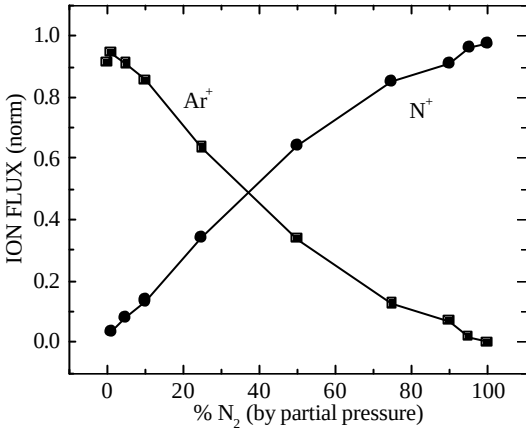

Figure 7 Normalized fluxes of dominant ions to a grounded stage for mixtures of Ar and N_2.

3. Results and Discussion

The photographs in Fig 2 illustrate the plasma localization, differences due to gas composition and the independence of the processing stage location in e-beam produced plasmas. Since the e-beam is the ionization source, the plasma is independent of the chamber and stage design (as long as the e-beam isn't intercepted). The visible light emission from the Ne plasma shows a diffusive nature of the emission while the N_2 plasma is strongly confined to the e-beam channel. Uniformity tests on this LAPPS are presently underway. The additional plasma characterizations shown in Fig 6 illustrate the plasma characteristics of very low electron temperatures, which result in a high density plasma with low plasma potentials and ion energies. From Fig 6, an abrupt peak in the electron temperature and the higher energy ion fluxes characterizes the ignition of the plasma, before the steady-state condition is reached.

The demonstrated reactive ion etching of polymer materials shows strong promise in terms of precise control of a typically isotropic, uncontrollable process that relies strongly on the desorption of carbon monoxide (CO) from the surface. From the data shown in Figs 3 and 4, etching of the resist material was an ion-driven process in an environment that contained an abundance of atomic oxygen neutrals. The direct

correlation between ion energy and material removal in Fig 3 shows that some ion energy was in fact necessary to remove material and the removal was not automatic (exothermic) in the presence of atomic oxygen (especially since the ER drops to nearly zero with no bias energy). In other plasma sources, organic material removal is considered a chemical process dependent only on the atomic oxygen flux to the surface. Thus, ion energy is not considered important in sources where the plasma potential exceeds 10 V. However, plasma potentials in e-beam produced plasmas are only 1-5 V, so initial ion energies are greatly reduced. Without some sort of additional activation (ion energy, temperature) the desorption of volatile etch species does not progress at measurable rates. This control of ion energy down to extremely low values provides additional benefits, as shown by the via residue removal in Figure 4. These test structures provided a much more rigorous test for process anisotropy and showed submicron feature evolution in an otherwise isotropic process. With only very fine (~ 50 nm) residues within small features, any process isotropy would quickly destroy the feature profile. Instead, a clean removal of the residuals left behind was seen, leaving the via structure intact. The results of Figure 3b suggest the plasma source produced a large reactive neutral flux, as the ER remained constant while the feedstock gas source of atomic oxygen was reduced. The ER was therefore not neutral-limited, until the molecular gas percentage fell below 20%.

The reactive ion etching of silicon also showed promising results in terms of material removal rates. At a moderate bias voltage of –125 V, the ER of ~ 1 micron/min for the Ar/SF_6 mixtures is comparable to other high density plasma etchers, although the ER for the O_2/SF_6 mixtures was much remarkably lower. Although the amount of SF_6 was lower in the O_2/SF_6 plasmas, the order of magnitude difference in ER at low energies was surprising, since a strong chemical etch component was expected. This lower ER is more indicative of a SiO_2 sputter yield at these energies, which is reasonable for the more dilute SF_6 plasmas. In this case, the flux of etchants was dominated by oxidizing species, which caused the surface to become more like SiO_2 prior to etching. In addition, the selectivity of SiO_2 over Si using SF_6 at these ion energies should be appreciable, although preliminary tests using an SiO_2 mask showed no selectivity in this plasma chemistry further suggesting SiO_x removal as the limiting step. The Ar/SF_6 plasma chemistry conversely showed a strong chemical and reactive ion etch components from 0-50 V and 50-150V, respectively, and then leveled out at the –275 V energy threshold.

While the present plasma nitriding experiments require further composition analysis, the results are impressive for an non-optimized plasma process. These growth rates are comparable with standard techniques[7] using rf and dc discharges, but the activation energy is low, making this process attractive from the thermal management standpoint. This low activation energy is believed to be due to the large fluxes of atomic nitrogen ions and neutrals produced in these plasmas. With the additional kinetic energy from the applied dc voltage, the atomic ions are the likely critical species for this process, considering that it is atomic nitrogen that adsorbs and diffuses into the bulk. These preliminary results along with the ion specie control demonstrated in Fig 7 makes the development of this process very lucrative from a materials standpoint.

Summary and Conclusion

Electron-beam produced plasmas were readily produced and used in various materials processing applications. The etching of photoresist in O_2/Ar chemistries demonstrated a high degree of control over a predominantly chemical process. This control is attributed to the low incident ion energy from the plasma source, which resulted in better ion energy control with an externally applied rf bias. Similarly, the silicon etching in O_2/SF_6 and Ar/SF_6 mixtures showed a stronger ion-driven component than expected. The limiting step in the O_2/SF_6 mixtures was the removal of an SiO_x layer, due to the large amounts of atomic oxygen generated by the plasma. The use of Ar/SF_6 mixtures eliminated the SiO_x layer as a limiting step and dramatically increased the Si etch rate, at both low and high ion energies. Further tests will focus on feature evolution and anisotropy of these etching conditions. The stainless steel nitriding experiments were encouraging, resulting in both high growth rates (~ 1 micron/hr) and low activation energy (85 kJ/mole), for a large area process. The fact that e-beam produced plasmas in diatomic gases supply predominantly atomic ions to the workpiece makes it an attractive system for plasma nitriding of materials.

The reactive ion etching and nitriding experiments discussed here were proof-of-concept tests for the practicality of applying e-beam produced plasmas to more widespread applications. In order to take full advantage of the versatility of these plasma sources, a more comprehensive design-of-experiments is necessary to optimize the processes. The fact that modulated plasmas offer additional process space not always accessible with continuous plasma sources is another area to be further explored. These plasma sources offer considerable flexibility for modifying materials, although only a few of the attributes have been

investigated thus far. The absence of high plasma electron temperatures (and therefore large plasma potentials) allows a variety of processing conditions without sacrificing flux of reactive charged or neutral species. This work demonstrated important attributes of ion energy control and damage-free etching possibilities, versatility of ion flux through gas composition, competitive nitriding rates and scalability within an actual plasma processing environment.

Acknowledgements

The authors gratefully appreciate the assistance of Dr. John Hallock (formerly of Axcelis Technologies, Rockville, MD) with the via structures. The technical assistance of Anthony Noll (NRL) and Robert Lanham (SFA, Inc., Lanham, MD) was also greatly appreciated. The Office of Naval Research supported this work.

References

[1] R. F. Fernsler, W. M. Manheimer, R. A. Meger, J. Mathew, D. P. Murphy, R. E. Pechacek and J. A. Gregor, *Phys. Plasmas* **5**, 2137 (1998).
[2] W. M. Manheimer, R. F. Fernsler, M. Lampe and R. A. Meger, *Plasma Sources Sci. Technol.* **9**, 370 (2000).
[3] D. Leonhardt, S. G. Walton, D. D. Blackwell, W. E. Amatucci, D. P. Murphy, R. F. Fernsler and R.A. Meger, *J. Vac. Sci. Technol. A* **19**, 1367 (2001).
[4] S. G. Walton, D. Leonhardt, D. D. Blackwell, D. P. Murphy, R. F. Fernsler and R. A. Meger, *J. Vac. Sci. Technol. A* **19**, 1325 (2001).
[5] D. Leonhardt, *Vacuum Technology and Coating* 24 (November 2001).
[6] D. Leonhardt, C. Muratore, S. G. Walton, D. D. Blackwell, R. F. Fernsler and R.A. Meger, submitted to *Surface Coatings and Technology*.
[7] D. L. Williamson, et al. *Surf. Coat. Technol.* **65**, 15 (1994); E. Menthe, K.-T. Rie, *Surf. Coat. Technol.* **116/119**, 199 (1999); M.P. Fewell, J. M. Priest, M. J. Baldwin, G. A. Collins, K. T. Short, *Surf. Coat. Technol.* **131**, 284 (2000).